International Journal of Enhanced Research in Science, Technology & Engineering
ISSN: 2319-7463, Vol. 8 Issue 10, October -2019, Impact Factor: 6.754

Contribution of added nanoparticles in the enhancement of the condensation on liquid film process inside a vertical steam condensers

Mustapha Ait Hssain[*1], Youness El Hammami[2], Rachid Mir[3]

[1,2,3]Laboratory of Mechanics, Processes, Energy, and Environment (LMPEE),
National School of Applied Sciences, Ibn Zohr University, Agadir, Morocco

ABSTRACT

In this study, the flow of the air-vapor-nanoparticle mixture is supposed to be laminar, stationary and two-dimensional. The coupled governing equations for liquid film, interfacial conditions and mixture flow are solved together using the finite volume method. Thus, the objective of this study is to analyze the effect of uniform injection of different types of nanoparticles on improving heat and mass transfer during condensation of water vapor in a vertical channel. The effect of operating conditions is also determined and carefully examined under the variation of relative humidity, inlet Reynolds number, inlet pressure, inlet temperature, cooling temperature and different types of nanoparticles (Cu , CuO , Al_2O_3, SiO_2, TiO_2 **). The results presented include temperature distribution, local Nusselt number of condensed film, local Sherwood number, liquid film thickness, and condensation rate. The results reveals that the effectiveness of the nano fluid becomes higher than that with the base fluid when the inlet Reynolds number, inlet relative humidity, and the inlet temperature are higher and when inlet pressure are lower.**

Keywords: **Condensation on film, nanoparticles, vertical channel, air-steam mixture, mixed convection, heat and mass transfer.**

1. INTRODUCTION

The processes of heat and mass transfer during film condensation flowing on vertical, horizontal or inclined walls have been the subject of many researches after the work of Nusselt [1]. Many authors have devoted their attention to improving and optimizing the film condensation phenomenon of humid air, this phenomenon is widely used in many applications such as air conditioning, hot gas filtration, coal combustion, heating systems, ventilation, chemical processing, heat exchangers, and cooling [2-8]. The recent development of nano-technological materials leads to improve heat transfer by using metal nanoparticles suspended in base fluids. Accordingly, the effect of the presence of nanoparticles in the vapor phase on the condensation phenomenon deserves to be deeply studied in order to understand the physical mechanisms that control the enhancement of heat and mass transfer following the addition of nanoparticles to basic fluid.

The number of publications devoted to the study of heat and mass transfer during condensation in the presence of nanoparticles remains rather limited, despite its importance in improving the efficiency of industrial processes. Nanofluids have become a new frontier for scientific research because of the higher thermo physical properties than those of the base fluid. Indeed, among the research works that have focused on the study of heat and mass transfer during condensation in the presence of nanoparticles we find: Andriy A. Avramenko et al. [9, 10] who carried out an analytical investigation of heat and mass transfer at the condensation of the stationary vapor with the presence of nanoparticles near a vertical[9] and horizontal [10]plate. The novelty of the mathematical model used in their work is the incorporation of an equation for nanoparticles concentration, which takes into account the Brownian and thermophoretic diffusion mechanisms. The results of this studies shows that an increase in the fraction of nanoparticles leads to a significant improvement in heat and mass transfer, which promotes condensation. Mustafa Turkyilmazoglu et al. [11] extended in their paper the classical Nusselt condensate falling film theory when the nanoparticles is added to the base fluid. The results indicate that the thickness of the liquid condensate film decreases with increasing heat transfer rate as more volume fraction of the nanoparticles are added. This is due to the acceleration of the flow inside the momentum boundary layer, ultimately leading to more heat being transferred to the outside.

El Mghari et al. [12] numerically studied heat transfer by nanofluid condensation inside a horizontal smooth channel. Their numerical results are compared with previous experimental predictions and show that the heat transfer coefficient

is improved by 20% by increasing the volume fraction of Cu nanoparticles by 5%.They also found that the total pressure drop increases by increasing the concentration of nanoparticles in the base fluid. This is explained by the increase in viscosity and density of the fluid following the increase in the concentration of Cu nanoparticles. Iman Zeynali Famileh et al. [13] numerically analyzed the effect of the use of nanoparticles on the improvement of film condensation of humid air at different relative humidities and input speeds in the presence of nanoparticles. For the conditions studied in their article, the use of nanoparticles improves the rate of condensation. Their results show also that an increase in the mass concentration of nanoparticles has a significant effect on the Reynolds number of the condensed film and on the Sherwood number, these effects are more important for higher relative humidity and higher velocity values. Malvandi et al. [14] focused on studying the condensation of nanofluids in downward film by considering in their model the migration effects of nanoparticles in the liquid film. Brownian motion and the Soret effect were taken into account in this study. These authors confirm that the Soret effect is the main mechanism of migration of nanoparticles to the cold wall through the liquid film. Experimentally, Qi Peng et al. [15] conducted an experimental analysis of R141b condensation in the presence of CuO nanoparticles with an average diameter of 40 nm in a vertical tube. Their results show that the condensation heat transfer coefficient is improved with the increase in nanoparticle concentration and steam mass flow. In addition, the increase in the degree of steam superheat leads to an increase in the thermal transfer coefficient.

In the present study, the effect of nanoparticles on water vapor film condensation in the presence of a non-condensable gas, for different types of nanoparticles and for different inlet flow parameters in a vertical channel, is studied and discussed. The equations for conservation of mass, momentum, and energy in the film and in the vapor–gas mixture as well as the diffusion equation for the mixture are solved using the finite volume method. The results presented in this study are in terms of local Nusselt number, local Sherwood number, accumulated condensation rate, liquid film thickness and effective improvement rate.

2. GOVERNING EQUATIONS

A. Physical model

Fig. 1 shows the schematic view of the studied channel which is a vertical channel with the cooled walls is maintained at a constant temperature. The flow arriving at the inlet of the channel is uniform consisting humid-air-nanoparticles mixture. It was assumed that the nanoparticles were injected uniformly at the inlet and with similar hydrodynamic and thermal conditions of the main stream. The encounter of this hot flow with the cooled walls of the channel causes the condensation of water vapor on the channel wall, the condensed film has a downward movement along the cooling wall due to the force of gravity (the only external force) and the interfacial friction forces. To simulate this problem, we consider a vapor of water with nanoparticles in the presence of non-condensable gas flowing inside a vertical channel of length L and whose distance between its walls is equal to 2H. This forms a parallel plate channel, which is symmetrical about the median plane as shown in Fig. 1.

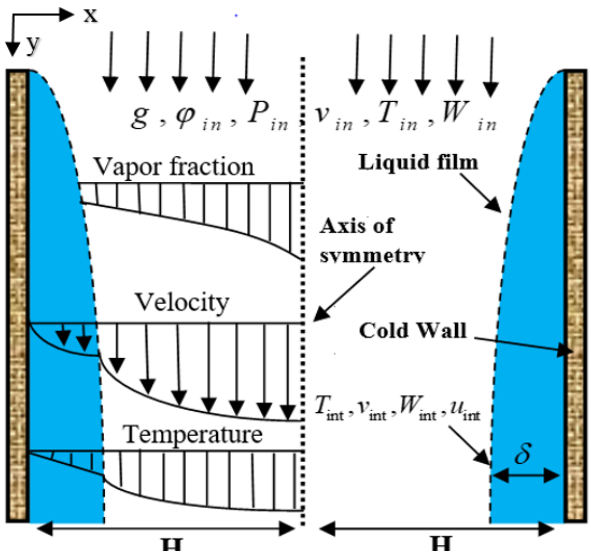

Figure 1: Schematic of the physical model study

In formulating the mathematical model, the following assumptions have been made:

- ★ The flow of liquid film and of vapor-gas mixture is considered laminar, two dimensional and stationary.
- ★ The vapor-air mixture is considered as an ideal mixture of water vapor and dry air.
- ★ The radiation heat transfer and the viscous dissipation terms are neglected in the energy equation.

- ★ The equilibrium condition exists at the interface liquid-vapor.
- ★ The Brownian and thermodiffusion mechanisms are neglected.
- ★ There is a local thermal equilibrium between nanoparticles and main flow.
- ★ The liquid film contains the same fraction of nanoparticle as in the vapor phase.

B. Liquid filmwith nanoparticles model

Considering the above mentioned assumptions, the equations in the liquid phase can be written as follows:

a) *Mass conservation:*

$$\frac{\partial}{\partial x}(\rho_{nf,L}u_{nf,L})+\frac{\partial}{\partial y}(\rho_{nf,L}v_{nf,L})=0 \quad (1)$$

b) *Momentum conservation:*

$$\frac{\partial}{\partial x}(\rho_{nf,L}u_{nf,L}u_{nf,L})+\frac{\partial}{\partial y}(\rho_{nf,L}v_{nf,L}u_{nf,L})=-\frac{\partial P_{nf,L}}{\partial x}+\frac{\partial}{\partial x}\left(\mu_{nf,L}\frac{\partial u_{nf,L}}{\partial x}\right)+\frac{\partial}{\partial y}\left(\mu_{nf,L}\frac{\partial u_{nf,L}}{\partial y}\right) \quad (2)$$

$$\frac{\partial}{\partial x}(\rho_{nf,L}u_{nf,L}v_{L})+\frac{\partial}{\partial y}(\rho_{nf,L}v_{nf,L}v_{nf,L})=-\frac{\partial P_{nf,L}}{\partial y}+\frac{\partial}{\partial x}\left(\mu_{nf,L}\frac{\partial v_{nf,L}}{\partial x}\right)+\frac{\partial}{\partial y}\left(\mu_{nf,L}\frac{\partial v_{nf,L}}{\partial y}\right)+\rho_{nf,L}g \quad (3)$$

c) *Energy conservation:*

$$\frac{\partial}{\partial x}(\rho_{nf,L}C_{P,nf,L}u_{nf,L}T_{nf,L})+\frac{\partial}{\partial y}(\rho_{nf,L}C_{P,nf,L}v_{nf,L}T_{nf,L})=\frac{\partial}{\partial x}\left(\lambda_{nf,L}\frac{\partial T_{nf,L}}{\partial x}\right)+\frac{\partial}{\partial y}\left(\lambda_{nf,L}\frac{\partial T_{nf,L}}{\partial y}\right) \quad (4)$$

C. Humid air with nanoparticles mixture model

Owing to the assumptions mentioned above, the equations of the mixture domain can be written as follows:

a) *Mass conservation:*

$$\frac{\partial}{\partial x}(\rho_{nf,M}u_{nf,M})+\frac{\partial}{\partial y}(\rho_{nf,M}v_{nf,M})=0 \quad (5)$$

b) *Momentum conservation:*

$$\frac{\partial}{\partial x}(\rho_{nf,M}u_{nf,M}u_{nf,M})+\frac{\partial}{\partial y}(\rho_{nf,M}v_{nf,M}u_{nf,M})=-\frac{\partial P_{nf,M}}{\partial x}+\frac{\partial}{\partial x}\left(\mu_{nf,M}\frac{\partial u_{nf,M}}{\partial x}\right)+\frac{\partial}{\partial y}\left(\mu_{nf,M}\frac{\partial u_{nf,M}}{\partial y}\right) \quad (6)$$

$$\frac{\partial}{\partial x}(\rho_{nf,M}u_{nf,M}v_{nf,M})+\frac{\partial}{\partial y}(\rho_{nf,M}v_{nf,M}v_{nf,M})=-\frac{\partial P_{nf,M}}{\partial y}+\frac{\partial}{\partial x}\left(\mu_{nf,M}\frac{\partial v_{nf,M}}{\partial x}\right)+\frac{\partial}{\partial y}\left(\mu_{nf,M}\frac{\partial v_{nf,M}}{\partial y}\right)+\rho_{nf,M}g \quad (7)$$

c) *Energy conservation:*

$$\frac{\partial}{\partial x}(\rho_{nf,M}C_{P,nf,M}u_{nf,M}T_{nf,M})+\frac{\partial}{\partial y}(\rho_{nf,M}C_{P,nf,M}v_{nf,M}T_{nf,M})=\frac{\partial}{\partial x}\left(\lambda_{nf,M}\frac{\partial T_{nf,M}}{\partial x}\right)+\frac{\partial}{\partial y}\left(\lambda_{nf,M}\frac{\partial T_{nf,M}}{\partial y}\right) \quad (8)$$

d) *Species conservation:*

$$\frac{\partial}{\partial x}(\rho_{nf,M}u_{nf,M}W)+\frac{\partial}{\partial y}(\rho_{nf,M}v_{nf,M}W)=\frac{\partial}{\partial x}\left(\rho_{nf,M}D\frac{\partial W}{\partial x}\right)+\frac{\partial}{\partial y}\left(\rho_{nf,M}D\frac{\partial W}{\partial y}\right) \quad (9)$$

It's important to mention that the physical properties of gas-vapor mixture and liquid phase are taken to be variable.

Where ρ, u, v, P, T, W, μ, C_P, D, λ and g are respectively, density, axial velocity, transverse velocity, pressure, temperature, vapor mass fraction, dynamic viscosity, specific heat capacity, mass diffusivity, thermal conductivity and gravitational acceleration. The Subscripts used in, int, L, M, V, sat, W, nf, f and p are respectively, inlet, interface, liquid, mixture, vapor, saturate, wall, nanofluid, base fluid and particle.

D. Coordinate transformation for both phases

A transformation of coordinates was made before discretization of the governing equations of the condensation, in order to overcome the non-uniformity of the physical domain due to variable liquid film thickness. The (x, y) coordinates were transformed to (η, χ) coordinates as follows:

$$y = \chi \text{ for } 0 \le y \le L$$
$$\eta = x/\delta \text{ for } 0 \le x \le \delta$$

$$\eta = (x-\delta)/(H-\delta)+1 \text{ for } \delta \le x \le H$$

Following the aforementioned change of variables, the governing equations are thus transformed as follows:

a) *Continuity equation in the liquid film*

$$\frac{1}{\delta}\frac{\partial\left(\rho_{nf,L}u_{nf,L}\right)}{\partial\eta}+\frac{\partial\left(\rho_{nf,L}v_{nf,L}\right)}{\partial\chi}=\frac{\eta}{\delta}\frac{\partial\delta}{\partial\chi}\frac{\partial\left(\rho_{nf,L}v_{nf,L}\right)}{\partial\eta} \tag{10}$$

b) *Momentum equation in the liquid film*

$$\begin{aligned}&\frac{1}{\delta}\frac{\partial\left(\rho_{nf,L}u_{nf,L}u_{n,L}\right)}{\partial\eta}+\frac{\partial\left(\rho_{nf,L}v_{nf,L}u_{nf,L}\right)}{\partial\chi}=-\frac{1}{\delta}\frac{\partial P_{nf,L}}{\partial\eta}+\frac{1}{\delta^2}\frac{\partial}{\partial\eta}\left(\mu_{nf,L}\frac{\partial u_{nf,L}}{\partial\eta}\right)\\&+\frac{\partial}{\partial\chi}\left[\mu_{nf,L}\left(\frac{\partial u_{nf,L}}{\partial\chi}-\frac{\eta}{\delta}\frac{\partial\delta}{\partial\chi}\frac{\partial u_{nf,L}}{\partial\eta}\right)\right]-\frac{\eta}{\delta}\frac{\partial\delta}{\partial\chi}\frac{\partial}{\partial\eta}\left[\mu_{nf,L}\left(\frac{\partial u_{nf,L}}{\partial\chi}-\frac{\eta}{\delta}\frac{\partial\delta}{\partial\chi}\frac{\partial u_{nf,L}}{\partial\eta}\right)\right]\\&+\frac{\eta}{\delta}\frac{\partial\delta}{\partial\chi}\frac{\partial\left(\rho_{nf,L}v_{nf,L}u_{nf,L}\right)}{\partial\eta}\end{aligned} \tag{11}$$

$$\begin{aligned}&\frac{1}{\delta}\frac{\partial\left(\rho_{nf,L}u_{nf,L}v_{nf,L}\right)}{\partial\eta}+\frac{\partial\left(\rho_{nf,L}v_{nf,L}v_{nf,L}\right)}{\partial\chi}=-\frac{\partial P_{nf,L}}{\partial\chi}+\frac{\eta}{\delta}\frac{\partial\delta}{\partial\chi}\frac{\partial P_{nf,L}}{\partial\eta}+\frac{1}{\delta^2}\frac{\partial}{\partial\eta}\left(\mu_{nf,L}\frac{\partial v_{nf,L}}{\partial\eta}\right)\\&+\frac{\partial}{\partial\chi}\left[\mu_{nf,L}\left(\frac{\partial v_{nf,L}}{\partial\chi}-\frac{\eta}{\delta}\frac{\partial\delta}{\partial\chi}\frac{\partial v_{nf,L}}{\partial\eta}\right)\right]-\frac{\eta}{\delta}\frac{\partial\delta}{\partial\chi}\frac{\partial}{\partial\eta}\left[\mu_{nf,L}\left(\frac{\partial v_{nf,L}}{\partial\chi}-\frac{\eta}{\delta}\frac{\partial\delta}{\partial\chi}\frac{\partial v_{nf,L}}{\partial\eta}\right)\right]\\&+\frac{\eta}{\delta}\frac{\partial\delta}{\partial\chi}\frac{\partial\left(\rho_{n,L}v_{nf,L}v_{nf,L}\right)}{\partial\eta}+g\rho_{nf,L}\end{aligned} \tag{12}$$

c) *Energy equation in the liquid film*

$$\begin{aligned}&\frac{1}{\delta}\frac{\partial\left(\rho_{nf,L}C_{P,nf,L}u_{nf,L}T_{nf,L}\right)}{\partial\eta}+\frac{\partial\left(\rho_{nf,L}C_{P,nf,L}v_{nf,L}T_{nf,L}\right)}{\partial\chi}=\frac{1}{\delta^2}\frac{\partial}{\partial\eta}\left(\lambda_{nf,L}\frac{\partial T_{nf,L}}{\partial\eta}\right)+\\&\frac{\partial}{\partial\chi}\left[\lambda_{nf,L}\left(\frac{\partial T_{nf,L}}{\partial\chi}-\frac{\eta}{\delta}\frac{\partial\delta}{\partial\chi}\frac{\partial T_{nf,L}}{\partial\eta}\right)\right]-\frac{\eta}{\delta}\frac{\partial\delta}{\partial\chi}\frac{\partial}{\partial\eta}\left[\lambda_{nf,L}\left(\frac{\partial T_{nf,L}}{\partial\chi}-\frac{\eta}{\delta}\frac{\partial\delta}{\partial\chi}\frac{\partial T_{nf,L}}{\partial\eta}\right)\right]\\&+\frac{\eta}{\delta}\frac{\partial\delta}{\partial\chi}\frac{\partial\left(\rho_{nf,L}C_{P,nf,L}v_{nf,L}T_{nf,L}\right)}{\partial\eta}\end{aligned} \tag{13}$$

The mass, momentum and energy balance equations for the gas phase, and the diffusion equation for the gas species are shown as follow:

a) *Continuity equation in the gas-vapor region*

$$\frac{1}{H-\delta}\frac{\partial\left(\rho_{nf,M}u_{nf,M}\right)}{\partial\eta}+\frac{\partial\left(\rho_{nf,M}v_{nf,M}\right)}{\partial\chi}=\frac{2-\eta}{H-\delta}\frac{\partial\delta}{\partial\chi}\frac{\partial\left(\rho_{nf,M}v_{nf,M}\right)}{\partial\eta} \tag{14}$$

b) *Momentum equation in the gas-vapor region*

$$\begin{aligned}&\frac{1}{H-\delta}\frac{\partial\left(\rho_{nf,M}u_{nf,M}u_{nf,M}\right)}{\partial\eta}+\frac{\partial\left(\rho_{nf,M}v_{nf,M}u_{nf,M}\right)}{\partial\chi}=-\frac{1}{H-\delta}\frac{\partial P_{nf,M}}{\partial\eta}+\frac{1}{(H-\delta)^2}\frac{\partial}{\partial\eta}\left(\mu_{nf,M}\frac{\partial u_{nf,M}}{\partial\eta}\right)\\&+\frac{\partial}{\partial\chi}\left[\mu_{nf,M}\left(\frac{\partial u_{nf,M}}{\partial\chi}-\frac{2-\eta}{H-\delta}\frac{\partial\delta}{\partial\chi}\frac{\partial u_{nf,M}}{\partial\eta}\right)\right]-\frac{2-\eta}{H-\delta}\frac{\partial\delta}{\partial\chi}\frac{\partial}{\partial\eta}\left[\mu_{nf,M}\left(\frac{\partial u_{nf,M}}{\partial\chi}-\frac{2-\eta}{H-\delta}\frac{\partial\delta}{\partial\chi}\frac{\partial u_{nf,M}}{\partial\eta}\right)\right]\\&+\frac{2-\eta}{H-\delta}\frac{\partial\delta}{\partial\chi}\frac{\partial\left(\rho_{nf,M}v_{nf,M}u_{nf,M}\right)}{\partial\eta}\end{aligned} \tag{15}$$

$$\frac{1}{H-\delta}\frac{\partial\left(\rho_{nf,M}u_{nf,M}v_{nf,M}\right)}{\partial\eta}+\frac{\partial\left(\rho_{nf,M}v_{nf,M}v_{nf,M}\right)}{\partial\chi}=-\frac{\partial P_{nf,M}}{\partial\chi}+\frac{2-\eta}{H-\delta}\frac{\partial\delta}{\partial\chi}\frac{\partial P_{nf,M}}{\partial\eta}$$
$$+\frac{1}{\left(H-\delta\right)^2}\frac{\partial}{\partial\eta}\left(\mu_{nf,M}\frac{\partial v_{nf,M}}{\partial\eta}\right)+\frac{\partial}{\partial\chi}\left[\mu_{nf,M}\left(\frac{\partial v_{nf,M}}{\partial\chi}-\frac{2-\eta}{H-\delta}\frac{\partial\delta}{\partial\chi}\frac{\partial v_{nf,M}}{\partial\eta}\right)\right] \quad (16)$$
$$-\frac{2-\eta}{H-\delta}\frac{\partial\delta}{\partial\chi}\frac{\partial}{\partial\eta}\left[\mu_{nf,M}\left(\frac{\partial v_{nf,M}}{\partial\chi}-\frac{2-\eta}{H-\delta}\frac{\partial\delta}{\partial\chi}\frac{\partial v_{nf,M}}{\partial\eta}\right)\right]+\frac{2-\eta}{H-\delta}\frac{\partial\delta}{\partial\chi}\frac{\partial\left(\rho_{nf,M}v_{nf,M}v_{nf,M}\right)}{\partial\eta}+g\rho_{nf,M}$$

c) *Energy equation in the gas-vapor region*

$$\frac{1}{H-\delta}\frac{\partial\left(\rho_{nf,M}C_{P,nf,M}u_{nf,M}T_{nf,M}\right)}{\partial\eta}+\frac{\partial\left(\rho_{nf,M}C_{P,nf,M}v_{nf,M}T_{nf,M}\right)}{\partial\chi}=\frac{1}{\left(H-\delta\right)^2}\frac{\partial}{\partial\eta}\left(\lambda_{nf,M}\frac{\partial T_{nf,M}}{\partial\eta}\right)$$
$$+\frac{\partial}{\partial\chi}\left[\lambda_{nf,M}\left(\frac{\partial T_{nf,M}}{\partial\chi}-\frac{2-\eta}{H-\delta}\frac{\partial\delta}{\partial\chi}\frac{\partial T_{nf,M}}{\partial\eta}\right)\right]-\frac{2-\eta}{H-\delta}\frac{\partial\delta}{\partial\chi}\frac{\partial}{\partial\eta}\left[\lambda_{nf,M}\left(\frac{\partial T_{nf,M}}{\partial\chi}-\frac{2-\eta}{H-\delta}\frac{\partial\delta}{\partial\chi}\frac{\partial T_{nf,M}}{\partial\eta}\right)\right] \quad (17)$$
$$+\frac{2-\eta}{H-\delta}\frac{\partial\delta}{\partial\chi}\frac{\partial\left(\rho_{nf,M}C_{P,nf,M}v_{nf,M}T_{nf,M}\right)}{\partial\eta}$$

d) *Diffusion equation in the gas-vapor region*

$$\frac{1}{H-\delta}\frac{\partial\left(\rho_{nf,M}u_{nf,M}W\right)}{\partial\eta}+\frac{\partial\left(\rho_{nf,M}v_{nf,M}W\right)}{\partial\chi}=\frac{1}{\left(H-\delta\right)^2}\frac{\partial}{\partial\eta}\left(\rho_{nf,M}D\frac{\partial W}{\partial\eta}\right)$$
$$+\frac{\partial}{\partial\chi}\left[\rho_{nf,M}D\left(\frac{\partial W}{\partial\chi}-\frac{2-\eta}{H-\delta}\frac{\partial\delta}{\partial\chi}\frac{\partial W}{\partial\eta}\right)\right]-\frac{2-\eta}{H-\delta}\frac{\partial\delta}{\partial\chi}\frac{\partial}{\partial\eta}\left[\rho_{nf,M}D\left(\frac{\partial W}{\partial\chi}-\frac{2-\eta}{H-\delta}\frac{\partial\delta}{\partial\chi}\frac{\partial W}{\partial\eta}\right)\right] \quad (18)$$
$$+\frac{2-\eta}{H-\delta}\frac{\partial\delta}{\partial\chi}\frac{\partial\left(\rho_{nf,M}v_{nf,M}W\right)}{\partial\eta}$$

E. Boundary conditions:

The boundary conditions in the transformed coordinates are detailed below:

- At the entrance of the canal $\chi=0$

$$v_{nf,L}=u_{nf,L}=u_{nf,M}=0. \quad ; \quad v_{nf,M}=v_{in} \quad ; \quad T_{nf,M}=T_{in} \quad ; \quad T_{nf,L}=T_W \quad ; W=W_{in} \quad (19)$$

- At the outlet of the canal $\chi=L$

$$\frac{\partial T_{nf,L}}{\partial\chi}=\frac{\partial T_{nf,M}}{\partial\chi}=\frac{\partial W}{\partial\chi}=\frac{\partial u_{nf,L}}{\partial\chi}=\frac{\partial u_{nf,M}}{\partial\chi}=\frac{\partial v_{nf,L}}{\partial\chi}=\frac{\partial v_{nf,M}}{\partial\chi}=0. \quad (20)$$

- On the left wall $\eta=0$

$$u_{nf,L}=0 \ ; \ v_{nf,L}=0 \ ; \ T_{nf,L}=T_W \quad (21)$$

- At the interface $\eta=1$

$$v_{nf,L,\text{int}}=v_{nf,M,\text{int}} \quad (22)$$

$$\frac{\mu_{nf,L}}{\delta}\frac{\partial v_{nf,L}}{\partial\eta}\bigg|_{\text{int}}=\frac{\mu_{nf,M}}{H-\delta}\frac{\partial v_{nf,M}}{\partial\eta}\bigg|_{\text{int}} \quad (23)$$

$$T_{nf,L,\text{int}}=T_{nf,M,\text{int}}=T_{sat} \quad (24)$$

$$J''_{\text{int}}=-\frac{\rho_{nf,M}D}{\left(1-W_{\text{int}}\right)\left(H-\delta\right)}\frac{\partial W}{\partial\eta}\bigg|_{\text{int}} \quad (25)$$

$$\frac{\lambda_{nf,L}}{\delta}\frac{\partial T_{nf,L}}{\partial\eta}\bigg|_{\text{int}}=\frac{\lambda_{nf,M}}{H-\delta}\frac{\partial T_{nf,M}}{\partial\eta}\bigg|_{\text{int}}-J''_{\text{int}}h_{fg} \quad (26)$$

$$\rho_{nf,L,\text{int}}\left(u_{nf,L,\text{int}}-v_{nf,L,\text{int}}\frac{d\delta}{d\chi}\right)=\rho_{nf,M,\text{int}}\left(u_{nf,M,\text{int}}-v_{nf,M,\text{int}}\frac{d\delta}{d\chi}\right)=J''_{\text{int}} \quad (27)$$

- On the axis of symmetry $\eta=2$

$$\frac{\partial T_{nf,M}}{\partial\eta}=0. \quad ; \quad \frac{\partial W}{\partial\eta}=0. \quad ; \quad u_{nf,M}=0. \quad ; \quad \frac{\partial v_{nf,M}}{\partial\eta}=0. \quad (28)$$

h_{fg} is Latent heat of condensation

F. Nanoparticles proprieties:

In this study the properties of nanofluids (condensate with nanoparticles and air-vapor-nanoparticles) are calculated as a function of the fraction of nanoparticles, the properties of solid nanoparticles as well as those of the base fluid. Thus, the properties of the nanofluid are obtained by the following relationships [16-17]:

$$\mu_{nf} = (1-\phi)^{-2.5}\,\mu_f \tag{29}$$

$$\rho_{nf} = (1-\phi)\rho_f + \phi\rho_p \tag{30}$$

$$C_{P,nf} = (1-\phi)C_{P,f} + \phi C_{P,p} \tag{31}$$

$$\lambda_{nf} = \lambda_f \frac{\lambda_p + 2\lambda_f - 2\phi(\lambda_f - \lambda_p)}{\lambda_p + 2\lambda_f + 2\phi(\lambda_f - \lambda_p)} \tag{32}$$

ϕ is the volume fraction of nanoparticle

It should be noted that the nanoparticles used in this study are: (CuO, Al_2O_3, TiO_2, Cu, SiO_2), Table 1 groups the different thermophysical properties of these nanoparticles [16, 18,19].

Table 1: Thermophysical properties of nanoparticles

Properties	CuO	Al_2O_3	TiO_2	Cu	SiO_2
$C_p\,(J/kg.K)$	561	765	686.2	385	745
$\rho\,(kg/m^3)$	6450	3970	4250	8933	2220
$k\,(W/m.K)$	76.5	40	8.9538	400	1.38

G. Characteristic variables

To analyze the heat and mass transfer during the condensation at the interface, the local Nusselt and Sherwood numbers, the accumulated condensation rate and the effective improvement rate are defined respectively by the equations from (33) to (36).

- Total Nusselt number

$$Nu_y = -\frac{(2H)\lambda_{nf,M}}{\lambda_f\,(H-\delta)(T_{\text{int}} - T_{bulk})}\left.\frac{\partial T_{nf,M}}{\partial \eta}\right|_{\text{int}} + \frac{J''_{\text{int}} h_{fg}\,(2H)}{\lambda_f\,(T_{\text{int}} - T_{bulk})} \tag{33}$$

$T_{bulk} = \int_{\delta}^{H} \rho_{nf,M} C_{P,nf,M} v_{nf,M} T_{nf,M}\,dx \Big/ \int_{\delta}^{H} \rho_{nf,M} C_{P,nf,M} v_{nf,M}\,dx$ is the Bulk temperature

- Accumulated condensation rate

$$Mr = -\int_0^y J''_{\text{int}}\,dy \tag{34}$$

- The effective ratio

$$R_{eff} = \frac{\text{parameter in the case of nanofluid}}{\text{parameter in the case of base fluid}} \tag{35}$$

- Local Sherwood number

$$Sh_y = \frac{(2H)\,J''_{\text{int}}\,(1-W_{\text{int}})}{\rho_{nf,M} D\,(W_{\text{int}} - W_{bulk})} \tag{36}$$

$W_{bulk} = \int_{\delta}^{H} \rho_{nf,M} v_{nf,M} W\,dx \Big/ \int_{\delta}^{H} \rho_{nf,M} v_{nf,M}\,dx$ is the bulk mass fraction of the mixture.

- Effective thermal improvement rate:

$$R_{eff,th} = \left.\int_0^L Nu_y\,dy\right|_{nanofluid} \Big/ \left.\int_0^L Nu_y\,dy\right|_{Humid-Air} \tag{37}$$

- Effective mass improvement rate:

$$R_{eff,m} = \left.\int_0^L J''_{\text{int}}\,dy\right|_{nanofluid} \Big/ \left.\int_0^L J''_{\text{int}}\,dy\right|_{Humid-Air} \tag{38}$$

3. NUMERICAL RESOLUTION

The finite volume method [20] was used for the discretization of equations (10)-(18) with the appropriate boundary conditions. In order to handle convective and diffusion terms, the power law scheme was employed. For the velocity-pressure coupling, the SIMPLE algorithm (Semi-Implicit Method for Pressure-Linked Equations) was used. The sweeping method line by line, with the algorithm of Thomas was used for the iterative resolution of the systems of equations. Steady-state solutions are obtained using under-relaxation techniques.

A. *Stability of the Calculation Scheme*

The physical model in coordinates (x, y) is transformed into a numerical model in coordinates (χ, η). Then, both liquid and gas regions becomes rectangular domains as shown in Fig. 2. Therefore, the variable position of the interface becomes a perfectly vertical straight line and parallel to the wall. The numerical domain was divided into non-uniform grids. The distribution of the nodes in both domains varies to obtain a suitable refinement in the liquid region near to the cold wall and close to the interface as well as at the inlet of the channel; in the same way in the region of the vapor-gas mixture the mesh is thinner close to the interface, the axis of symmetry, and the entry of the channel as presented previously in Fig. 2. A study of the influence of the mesh on the variation of the local Nusselt number and condensed mass flow rate was conducted at different sections of the channel to determine the optimal mesh. The results obtained show that in the case of $NM = 51$, $NL = 21$, $NY = 901$ the relative error in the local Nusselt number and the condensed mass flow rate between the different grids tested does not exceed 0.6% and 0.7% respectively when compared with the finer grid. These differences are considered suitably small, so that grid was used for all the results presented in this work.

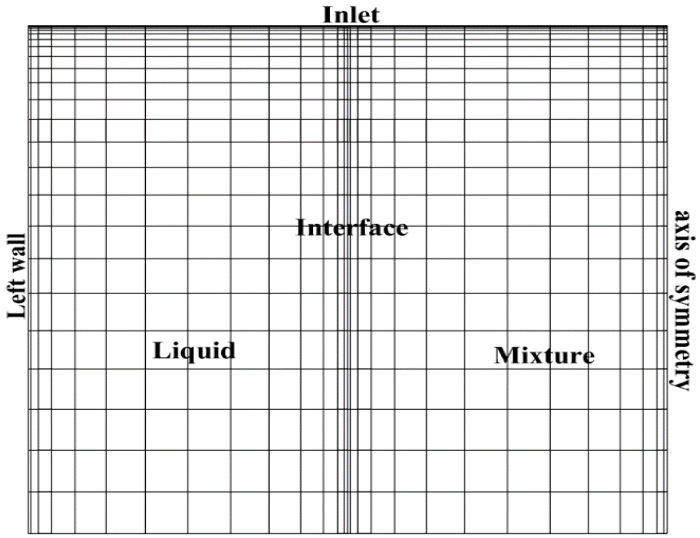

Figure 2: Schematic of the numerical model study

B. *Validation of numerical code*

The calculation code developed for the implementation of the numerical model described above is validated by checking the concordance of the numerical results obtained in the case of isothermal vertical wall channel by comparing with results obtained by other authors based on previous work in the literature. Two series of tests are performed, we compared our results with the experimental results of Levedev et al. [21] and the numerical results of Asis GIRI et al. [6]. The experimental study of [21] consist to analyze the heat transfer throughout condensation in an asymmetrically cooled channel, of width $H = 0.02m$ and the inlet numbers of Reynolds $\mathrm{Re}_{in} = 730$ and $\mathrm{Re}_{in} = 1460$. Fig. 3 shows the comparison between the heat transfer coefficient as a function of the specific humidity found by [21] and that found by the present model. Concerning the numerical study, AsisGiri et al. [6] are studied mixed convection heat transfer with condensation in a parallel plate channel, with details data below: $L = 0.75m$, $H = 0.005m$, $T_{in} = 60°C$, $T_W = 30°C$, $RH_{in} = 100\%$. Results of [6] are compared with present results in Fig. 4.

A very satisfactory agreement was observed between the results of the current model and those of the literature [21] and [6]. The small differences observed between our results and those of the AsisGiri et al. [6] can be attributed to mathematical models used.

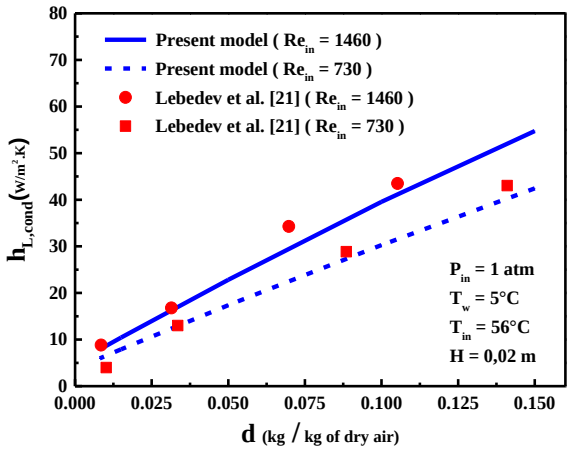

Figure 3: Validation with Lebedev et al. [21]

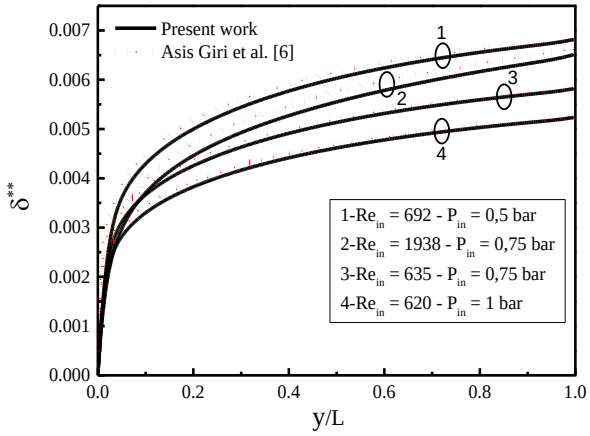

Figure 4: Validation with AsisGiri et al. [6]

4. RESULTS AND DISCUSSION

The effects of the type of nanoparticles on the heat and mass transfer enhancement during condensation of humid air are analyzed. Five types of nanoparticles are considered in the present study namely, alumina (Al_2O_3), Titania (TiO_2), Copper oxide (CuO), Silicon dioxide (SiO_2), and copper (Cu). The thermophysical characteristics of chosen different nanoparticles are listed in Table 1. The influence of the addition of nanoparticles on the condensation of moist air depends on the input conditions such as the nature of the nanoparticles used and the operating settings.

To distinguish the effect of these parameters, the Nusselt and Sherwood numbers and the thickness of the liquid film as well as the accumulated condensation rate along the channel are studied. It should be noted that the nanoparticles volume fraction is supposed fixe and equal to $\phi = 0.1\%$. This concentration is chosen very low to be easily mixed with moist air in order to avoid undesirable effects on the condensation phenomenon.

A. *Condensation of vapor with different types of nanoparticles*

The use of nanoparticles in the vapor phase mainly affects the thermophysical characteristics of the mixture (diluted nanoparticles with non-condensable gas), this effect can lead to an improvement in thermophysical properties that leads to a better condensation of moist air. To highlight the effect of the type of nanoparticles used, we examined different types of nanoparticles with different thermophysical properties listed in table 1.

The thickness of the liquid film is defined as the thermal resistance of the heat transfer between the vapor phase and the heat exchange surface. Fig. 5 shows the influence of the type of nanoparticles on heat and mass transfer during water vapor condensation in the presence of solid nanoparticles. For the same volume fraction of nanoparticles $\phi = 0.1\%$ and for fixed input parameters, we see from Fig. 5.a that in the inlet zone, the difference between the temperature of the wall and that of the vapor-air-nanoparticles mixture causes the condensation of the vapor on the channel walls. Indeed, the film thicknesses of the condensate have steep axial slopes due to the high vapor concentration gradient near the channel inlet (high initial condensation rate), followed by more moderate growth towards the outlet of the channel.

This trend is the same for all types of nanoparticles tested. In addition, the largest condensate film is obtained for the fluid with Cu nanoparticles because the latter have the highest density and also the highest thermal conductivity among the other nanoparticles tested. This figure also shows that the amount of vapor that condenses on the channel walls varies with the type of the nanoparticles used, while maintaining the other parameters fixed, so that nanoparticles with high density and high thermal conductivity allow better mass transfer as shown by the comparison between the condensate thicknesses.

The accumulated condensation rate, the Nusselt and Sherwood numbers along the channel are presented in Figures 5.b-c-d, these parameters have allowed to understand the influence of the properties of the added nanoparticles on mass transfer (Figures 5.b and 5.c) and on the total heat transfer (Figure 5.d). For the same input data, a comparison of the accumulated condensation rate of pure humid air and humid air with nanoparticles (Figure 5.b) shows that the use of nanoparticles improves the mass transfer coefficient that accelerates the condensation rate along the flow.

An adding of 0.1% of nanoparticles, increases the accumulated condensation rate by 807% and 208% respectively for Cu-nanoparticles and SiO2-nanoparticles the lowest thermal conductivity. Figure 5.d illustrates the profiles of the local Nusselt number obtained for different types of nanoparticles. The Nusselt number decreases sharply and rapidly near the entrance due to the presence of a strong temperature gradient that leads to a strong thermal boundary layer.

The effect of nanoparticles is perfectly clear in this region, the nanofluid with the better thermal conductivity has very high Nusselt values compared to others. Far from the entry region, the local Nusselt number reaches a fully developed regime, for all the nanoparticles studied, due to the reduction in heat removal capacity because of the decrease in condensation rates. In order to evaluate the contribution of nanoparticles on mass transfer, the local Sherwood number is presented in Fig. 5.c. The results show the influence of nanoparticles on improving the mass flow of steam to the condensed liquid film. We can see that nanoparticles increase the Sherwood number by about 20% in the case of Cu and by about 10% in the case of SiO_2 at the channel entrance. Based on these last two percentages of improvement, it can be concluded that the addition of nanoparticles improves mass transfer.

The operating conditions: $\mathrm{Re}_{in} = 1000$; $P_{in} = 1atm$; $\Delta T = 20^{\circ}C$; $T_{in} = 40^{\circ}C$; $H = 0.0125m$; $L = 1m$; $\phi = 0.1\%$

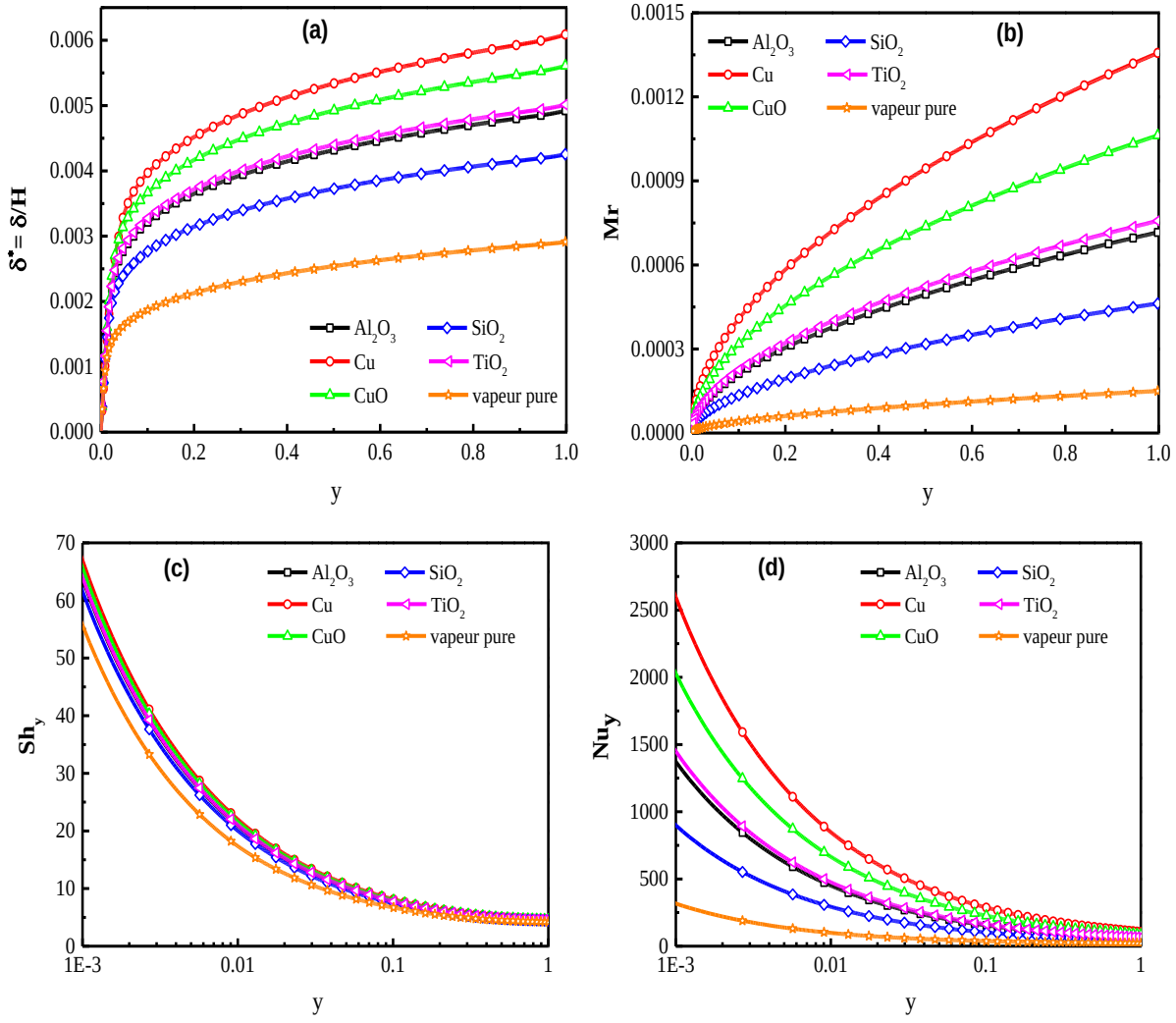

Figure 5: Influence of the nanoparticle type on the variation of (a) the thickness of the liquid film, (b) the condensation rate, (c) the local Sherwood number and (d) the local Nusselt number

B. *Effective improvement rate of heat and mass transfer*

To quantitatively evaluate the contribution of each type of nanoparticles added to the base fluid, we plotted the effective rate of improvement of heat and mass transfer which are characterized by the ratio of the total number of Nusselt and the ratio of the total condensation rate along the channel for the flow with nanoparticles to that without nanoparticles (37) and (38). Indeed, to highlight the influence of the different operating parameters of the system we have plotted these improvement rates for different inlet pressures Figs. 6.a and 6.b, inlet velocities Figs. 7.a and 7.b, inlet temperatures figs. 8.a and 8.b, wall cooling temperatures Figs. 9.a and 9.b and inlet relative humidities Figs. 10.a

and 10.b. From these figures we notice that the rate of improvement is higher than 1 ($R_{eff,th} > 1$ and $R_{eff,m} > 1$) for all the cases studied, this means that condensation in the presence of nanoparticles is better than condensation without nanoparticles.

This increase differs from one type of nanoparticle to another, it is more intense for Cu and CuO nanoparticles, which have very high properties compared to other nanoparticles, more precisely these particles have high density and high thermal conductivity which improves the properties of the air-vapor mixture thus leading to significant heat and mass exchanges justified by the improvement rates which reaches in some cases $R_{eff,m} = 17$ Fig. 6.a and $R_{eff,th} = 14$ for added Cu nanoparticles Fig. 6.b.

The graphs in Figs. 6.a and 6.b illustrate respectively the effective thermal and mass improvement rate as a function of the type of nanoparticles added for different inlet pressures. From these figures, we have reported that when the inlet pressure increases, the condensation potential decreases so that the vapor fraction decreases and the amount of non-condensable gas increases, which constitutes a resistance to mass transfer at the interface. Moreover, for the same inlet pressure, the use of nanoparticles is always favorable to increase the quantity of condensed steam. In general, when the pressure increases, the effective improvement rate decreases considerably for all types of nanoparticles.

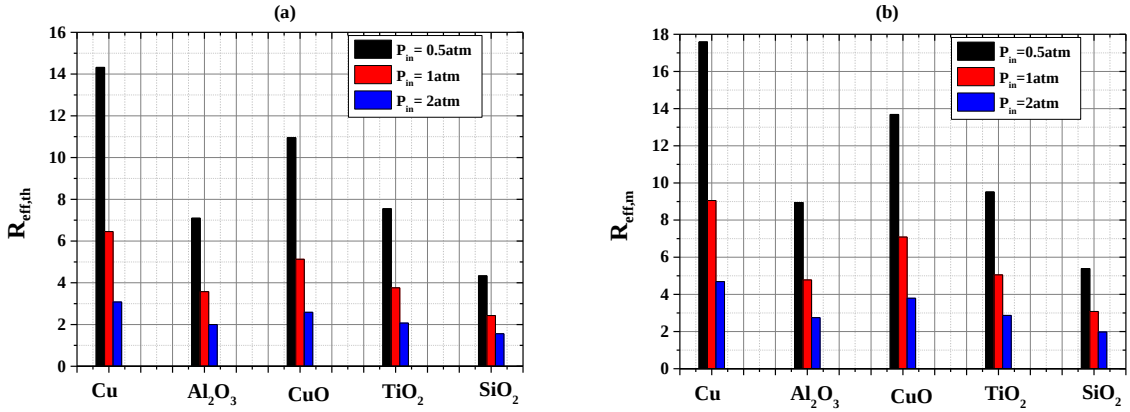

Figure 6: Thermal and mass improvement rates for different type of nanoparticles at different inlet pressure.

To analyze the effect of the increase in the inlet Reynolds number, $Re_{in} = 2\rho_{f,in} v_{f,in} H / \mu_{f,in}$, on the improvement of thermal and mass transfer, Figs. 7.a and 7.b present the variation in the rate of effective improvement according to the types of nanoparticles used and for different Reynolds numbers. By increasing the Reynolds number from $\mathrm{Re}_{in} = 500$ to $\mathrm{Re}_{in} = 2000$ the convection becomes more intense which increases the amount of condensed steam. This is true for all types of nanoparticles added to the base fluid but it is more pronounced in the case of Cu-nanoparticles compared to other types. It should be noted that the nanoparticles has a strong potential for improvement of phase change performance.

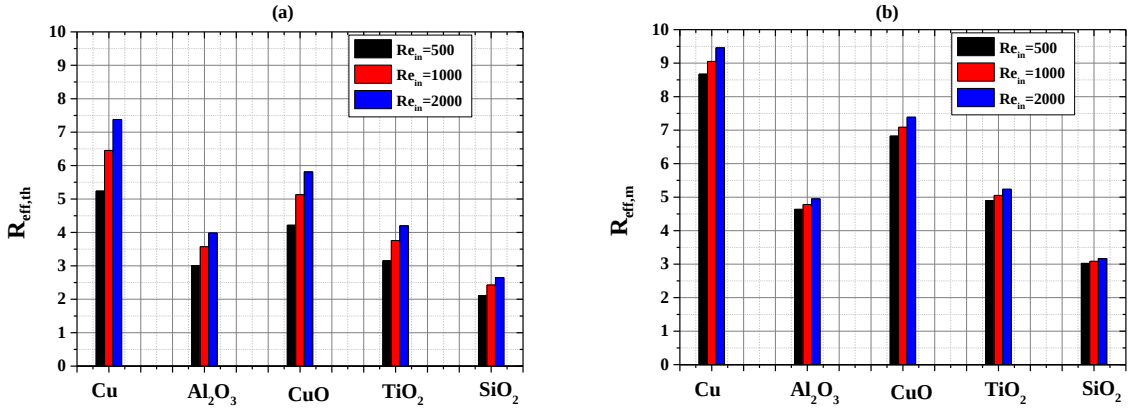

Figure 7: Thermal and mass improvement rates for different type of nanoparticles at different inlet Reynolds.

Figs. 8.a and 8.b show the variation in the thermal and mass effective improvement rate as a function of the mixture inlet temperature for different types of nanoparticles. From these figures, we observe that the increase in inlet temperature has a positive effect on heat and mass transfers. When the temperature of the inlet solution increases, the inlet vapor fraction increases also as the inlet pressure is maintained constant. Therefore, the diffusion force of the vapor to the liquid film increases and causes an increase in the mass flow through the interface. This trend is the same with all types of nanoparticles added.

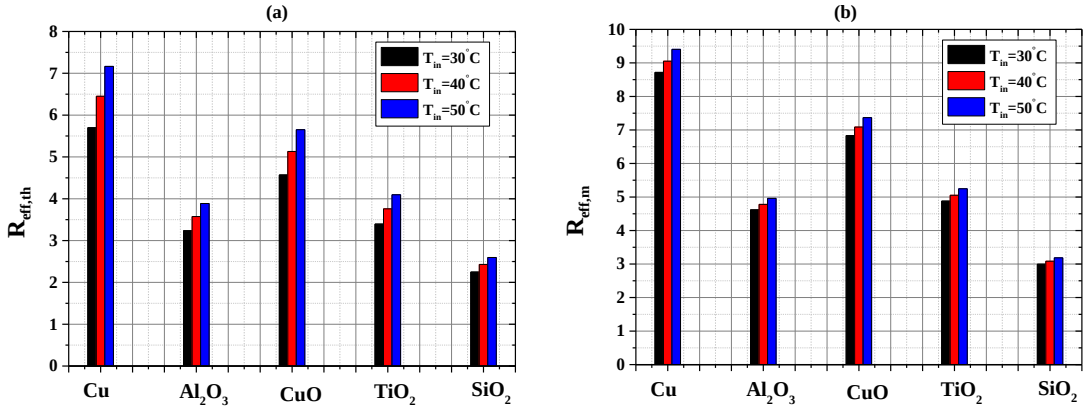

Figure 8: Thermal and mass improvement rates for different type of nanoparticles at different inlet temperature.

By analyzing the values of thermal improvement rate and mass presented in Figs. 9.a and 9.b, we can see that the influence of nanoparticles on condensation is better when the temperature difference between the wall and the inlet is small. This effect is the same for all types of nanoparticles tested with amplitude differences due to differences in the physical properties of nanoparticles. The figures also indicate that by adding the nanoparticles, the increase in T_W with fixed P_{in} , W_{in} and Re_{in} would result in an increase in the mass flow of liquid condensate at the interface along the channel. This is due to the better thermal conductivity of the nanoparticles, which allows more heat to be evacuated to the outside, thus promoting condensation.

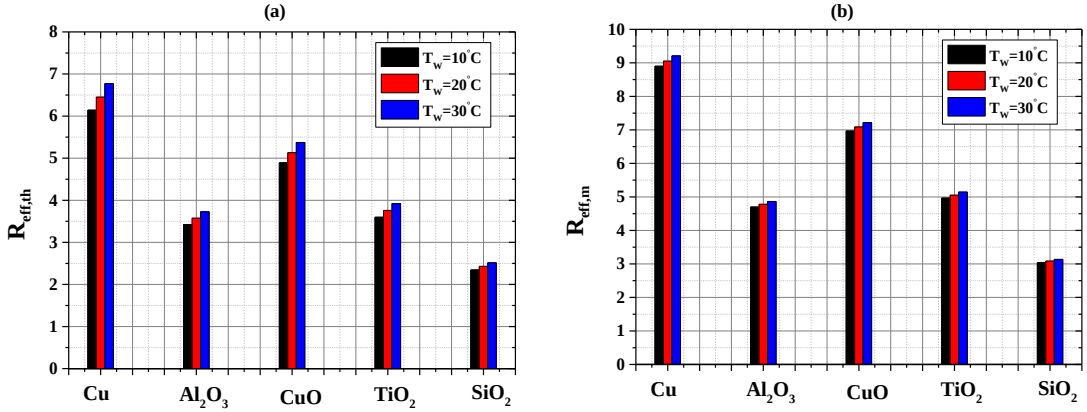

Figure 9: Thermal and mass improvement rates for different type of nanoparticles at different wall temperature.

The effect of relative humidity on condensation parameters is studied for water vapor-air with nanoparticles and the results are presented for different types of nanoparticles. Figs. 10.a and 10.b show the variation in the rate of thermal and mass enhancement, we can note that for each type of added nanoparticles the increase in the humidity of the main stream with a fixed temperature and inlet pressure consists in reducing the quantity of non-condensable gas in the main stream which leads to more condensed vapor, this result is confirmed by Fig. 10.a which illustrates that the rate of improvement increases as the humidity increases. In addition, the Cu-nanoparticles have higher improvement rates than other types. On the other hand, Fig. 10.b illustrates that the effect of nanoparticles on mass transfer is almost the same for all moisture values tested.

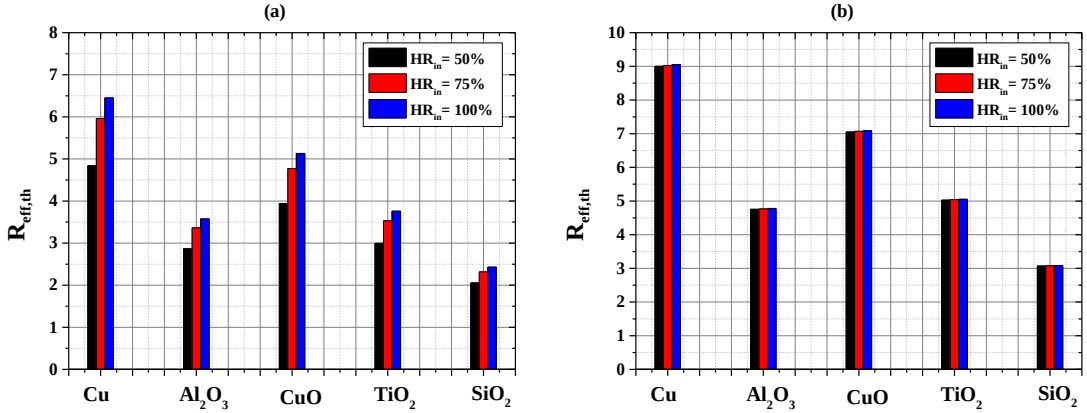

Figure 10: Thermal and mass improvement rates for different type of nanoparticles at different inlet relative humidity.

CONCLUSIONS

We studied numerically the effect of different type of nanoparticles on heat and mass transfer during the condensation of water vapor in the presence of the non-condensable gas along a vertical channel. The governing equations in the liquid film and the gas-vapor mixture are discretized by the finite volume method. A validation test of numerical model was also made. The main conclusions drawn from this study are summarized below:

- The accumulated condensation rate is enhanced with addition of nanoparticles by $R_{eff} = 8.07$ and $R_{eff} = 2.08$ respectively for Cu-nanoparticles and SiO_2-nanoparticles.
- The improvement in mass transfer characterized by Sherwood number is about 20% in the case of Cu-nanoparticles and is about 10% in the case of SiO2-nanoparticles at the channel inlet.
- The nanofluid which has a high thermal conductivity and high density leads to significant heat and mass exchanges which reaches in some cases $R_{eff,m} = 17$ and $R_{eff,th} = 14$ for added Cu nanoparticles.
- The condensation rate in the presence of nanoparticles increases with increasing inlet temperature T_{in} , inlet Reynolds number Re_{in} , inlet relative humidity RH_{in} and also with decreasing inlet pressure P_{in} and inlet-to-wall temperature difference ΔT .

REFERENCES

[1]. W. Nusselt. The condensation of steam on cooled surfaces (Traduit par D. Fullarton), Zeitschrift des Vereines Deutscher Ingenieure, Vol . 60, n. 27, pp. 541-575, 1916.
[2]. Y. El Hammami, M. Feddaoui, T. Mediouni, A. Mir, Numerical study of condensing a small concentration of vapour inside a vertical tube, Heat Mass Transfer 48 (9) 1675–1685. 2012.
[3]. Ait Hssain, M., El Hammami, Y., Mir, R., Armou, S., & Zine-Dine, K. (2019). Numerical Analysis ofLaminar Convective Condensation with the Presence of Noncondensable Gas Flowing Downward in aVertical Channel. Mathematical Problems in Engineering, 2019.
[4]. E.C. Siow, S.J. Ormiston, H.M. Soliman, A two-phase model for laminar film condensation from steam-air mixtures in vertical parallel-plate channels, Heat and Mass Transfer 40, pp. 365-375, 2004.
[5]. E.C. Siow, S.J. Ormiston, H.M. Soliman, Two-phase modelling of laminar film condensation from vapour–gas mixtures in declining parallel-plate channels, International Journal of Thermal Sciences 46, pp. 458–466, 2007.
[6]. Asis Giri, Dipanka Bhuyan, Biplab Das, A study of mixed convection heat transfer with condensation from a parallel plate channel, International Journal of Thermal Sciences 98, pp. 165-178, 2015
[7]. V. Dharma Rao, V. Murali Krishna, P.K. Sharma, K.V. Sharma, Convective condensation of vapour in laminar flow in a vertical parallel plate channel in the presence of a high concentration non-condensable gas, J. Heat Transf. 131, 011502-1-7. 2009.
[8]. Agrawal N, Das SK. Numerical studies on hydrogen distribution in enclosures in the presence of condensing steam. J Heat Transf 2015;137:121008.
[9]. Avramenko, Andriy A., et al. "Heat transfer at film condensation of stationary vapor with nanoparticles near a vertical plate." *Applied Thermal Engineering* 73.1 (2014): 391-398.
[10]. Avramenko, A. A., et al. "Heat transfer in stable film boiling of a nanofluid over a vertical surface." International Journal of Thermal Sciences 92 (2015): 106-118.
[11]. Turkyilmazoglu, Mustafa. "Analytical solutions of single and multi-phase models for the condensation of nanofluid film flow and heat transfer." *European Journal of Mechanics-B/Fluids* 53 (2015): 272-277.
[12]. El Mghari, H., H. Louahlia-Gualous, and E. Lepinasse. "Numerical study of nanofluid condensation heat transfer in a square microchannel." *Numerical Heat Transfer, Part A: Applications* 68.11 (2015): 1242-1265.
[13]. Famileh, Iman Zeynali, Javad Abolfazli Esfahani, and Kambiz Vafai. "Effect of nanoparticles on condensation of humid air in vertical channels." *International Journal of Thermal Sciences* 30 (2016).
[14]. Malvandi, A., D. D. Ganji, and I. Pop. "Laminar filmwise condensation of nanofluids over a vertical plate considering nanoparticles migration." Applied Thermal Engineering 100 (2016): 979-986.
[15]. Peng, Qi, et al. "Experimental investigation on flow condensation of R141b with CuO nanoparticles in a vertical circular tube." Applied Thermal Engineering 129 (2018): 812-821.
[16]. Oztop, Hakan F., and Eiyad Abu-Nada. "Numerical study of natural convection in partially heatedrectangular enclosures filled with nanofluids." International journal of heat and fluid flow 29.5 (2008):1326-1336.
[17]. X. Zhang, H. Gu, M. Fujii, Effective thermal conductivity and thermal diffusivity of nanofluids containing spherical and cylindrical nanoparticles, J. Appl. Phys. 100 (2006) 044325.
[18]. S. Kakac, A. Pramuanjaroenkij, Review of convective heat transfer enhancementwith nanofluids, Int. J. Heat Mass Transfer 52 (2009) 3187–3196.
[19]. M. Turkyilmazoglu, Exact analytical solutions for heat and mass transfer ofMHD slip flow in nanofluids, Chem. Eng. Sci. 84 (2012) 182–187.
[20]. S.V. Patankar, Numerical Heat Transfer and Fluid Flow, Hemisphere, Washington, DC, 1980.
[21]. P. Lebedev, A. Baklastov, Z. Sergazin, Aerodynamics, heat and mass transfer in vapour condensation from humid air on a at plate in a longitudinal ow in asymmetrically cooled slot, Vol. 12, 1969, pp. 833-841.